CHAPTER 137

FIELD AND MODEL DATA OF SPREADING IN ESTUARIES F. $Ohlmeyer^1$, D. $Berndt^2$

INTRODUCTION

The coastal regions in the highly industrialized zones of western Europe and other comparable parts of the world are a preferable field of new industrial settling. The economic reasons are: 1. Situation on deep water reachable by big vessels and 2. The increasing of the units of power plants and chemical industries demands for great quantities of water. For instance 200 up to $500 \text{ m}^3/\text{s}$ are no longer utopic today. Generally such great quantities are not available but in coastal regions especially on estuaries where the water movement is governed mainly by tidal action. Fig. 1 shows new industries and power plants in the region of the German Bay the shaded areas are consisting tidal models.

In order to avoid environmental damages by pollution of industrial or thermal wastes and to diminish the recirculation effects of power plant, it is necessary to get correct information of the concentration rates resp. temperatures that will appear in these regions.

The ways to get this information are well-known: 1. Direct measurements in prototype, 2. Mathematic models, 3. Hydraulic models or hybride models. Direct measurement is to some degree a necessary presumption to the latter two ways, but furthermore it afterwards gives information of the accordance of the model predictions. But often there is no money to do so.

Of course it is not necessary to measure the whole area that would mean model investigations scaled 1:1 - but some specific data will be sufficient.

1)	DiplIng.) Bundesanstalt	für Wasserbau
2)	Dipllng.) Hamburg,	Germany

COASTAL ENGINEERING

Such comparisons could be made by the Bundesanstalt für Wasserbau, Fed.Rep. of Germany, who carried out model investigations and field measurements in estuaries of the Elbe and the Ems which belong to the well mixed types with a tidal range of 2.5 up to 3.5 m.

RECIRCULATION EFFECTS

One subject of investigation was the recirculation of cooling water. Fig. 2 shows the scheme of the thermal circuit; during half a tidal cycle recirculation is nearly unavoidable. The temperature rise was in one case about 5°C, where the heat output at the condenser was $\Delta T_0 = 10^{\circ}$ C. The recirculation rate $g = \frac{\Delta Ti}{\Delta T_0}$ (ΔT_i is the temperature rise at the intake after the first cycle) can be expressed as $g = \frac{g_{\infty}}{1+g_{\infty}}$ where $g_{\infty} = \frac{\Delta Ti}{\Delta T_0}^{\infty}$ and $\Delta T_{i\infty}$ is the maximum possible temperature rise. For $\Delta T_{i\infty} = 5^{\circ}$ C, g = 0,33 results. This relation is derived from the geometrical progression $g_{\infty} = \sum_{i=1}^{\infty} g_i^{\alpha}$.

The recirculation rates can also be regarded as a mixing factor. The temperature curves (Fig. 3) show two peaks which appear just after and before slack tide respectively when the longitudinal flow velocity in the ambient estuary water approaches zero, and thus the lateral spreading becomes dominant. Without mixing there would be complete recirculation ($g \approx 1$).

With the aid of model investigations it could be achieved to diminish the recirculation rate of a power plant from 0.52 to 0.23 i.e. more than 50 %. The solution was a sheetpiling of 30 m length beneath the outlet structure. The situation of the inlet and outlet structures is shown in Fig. 4, a bird's view picture of the power plant in model. From left to right: inlet, outlet of the nuclear station; inlet, outlet of the oil fired station.

In order to seperate the influence of one power plant to the other, Rhodamine-B-Tracer was used. By this way the influence of the indirect recirculation from earlier tidal cycles could be eliminated too.

2358

SPREADING MECHANISM

During the slack tide, a remarkably large lateral spreading can be observed which apparently is caused by larger initial jet spreading. Therefore the plume of the pollutant shows a special shape which is depicted in Fig. 5. Fig. 6 demonstrates the enlargement of the plume at lower fluvial velocities. But the lateral spreading in a free stream is also substantially larger during the slack tide than in times of a higher velocity, and originates from intensified convective lateral transport, resulting from large volume eddies. The interaction between convection and turbulent diffusion largely governs the spreading process in the tidal region.

MODEL INVESTIGATIONS

A good accordance between model and prototype presumes a correct simultation of the velocity field as well as a fairly good turbulent diffusion all over the tidal cycle.

The latter is only possible with a specific distortion, where the depth scale has to be

$$\lambda_2 = \lambda_1^{3/4}$$

relation of distortion for turbulent flow in the rough region λ_{\star} = length scale

This relation is derived, with the aid of dimensional analysis, from Kolmogoroff's equation (1), the turbulent diffusion equation (2) and the roughness condition $\lambda_{\tau} = 1$ through the application of the Manning-Strickler formula (3) valid for turbulent flow in the rough region (Reynolds' Number Re > 1200).

(1)
$$E = c \cdot G^{4/3} \cdot \ell^{4/3}$$

(Kolmogoroff)
E = diffusion coefficient
G = energy dissipation per unit
 mass
ℓ = characteristic length of eddies

c = a constant

$$(2) \qquad \frac{\Im c}{\Im t} + u \frac{\Im c}{\Im x} + v \frac{\Im c}{\Im y} = \frac{\Im}{\Im x} \Im \left(D_x \frac{\Im c}{\Im x} \right) + \frac{\Im}{\Im y} \Im \left(D_y \frac{\Im c}{\Im y} \right)$$

(3) $u = \frac{4}{n} R^{\frac{2}{3}} J^{\frac{1}{3}}$ (Manning-Strickler)

The energy dissipation and the turbulent friction are in this region only dependent upon $\frac{h}{d}$ (h = roughness height), (d = depth), i.e. geometric parameters that are easily to simulate in the model. Models scaled 1:100 (depth) and 1:500 (length and width) fullfill this condition und have shown good results.

COMPARISON OF MODEL DATA WITH MEASUREMENT IN PROTOTYPE

Various field measurements were performed to verify model experiments on lateral spreading of the polluted plume. Fig. 7 shows the lateral distribution of the spreaded plume 1 1/2 hours before low water, 90 m below the outlet, 3 m under the surface (near field test). Temperatures as well as concentrations rates of Rhodamine were measured in prototype and model. To indicate Rhodamine concentration a Turner Fluorometer was used. The field results are almost identical with the model results. Comparisons between the spreading of a dye patch in prototype and model is shown by the graph on Fig. 8 (far field test). Fig. 9 depicts the dye patch of Rhodamine from an airplane.

The recording of time dependent temperature or concentration values has been shown to be advantageous for the estimation of the effect of an inflow (Fig. 10), since here maximum and minimum values are recorded. By this way it is possible to separate the influence from earlier tides. The oscillation is due to tidal action only and after 5 to 10 tidal periods there will be an equilibrium.

APPLICABILITY OF PHYSICAL MODELS

It can be confirmed by comparison between model and prototype data that it is possible to simulate not only the dispersion in the far field area where the mixing process is governed by free turbulent structures and the velocity

SPREADING IN ESTUARIES

field of the stream but also the initial spreading of the penetrating jet in the near field and the transition zone. In this region it is necessary to record the width of the polluted plume in the correct way at all tidal phases. This is possible by using artificial roughness elements at the outlet point.

In addition to the report of Dr. Schwarze (7.3.) one should point out, that the distortion of the model is not only a good thing in simulating thermal losses (thermal decay) but besides it is a necessary presumption of recording the dispersion process in a physical model. The choice of scales is not free but fixed to a specific relation.

The usage of the "characteristic length" in Kolmogoroff's equation in passage 4 is only a mere thing of comparison without knowing the real value of it. It is used only in the dimensionless sense in the applicated analysis. In reality the "characteristic length" is equal to the diameter of the largest eddies, which may fill the width of the stream.

DECAY OF A POLLUTANT

Waste water, radioactive pollutants and cooling water are subject to decay. This decay can't be simulated in the physical model if one is using a conservative tracer. But there is a method to calculate this decay when getting the concentration rates due to the mere spreading process of turbulent diffusion and convection from the model.

Furthermore, a decay curve has to be known (Fig. 11). According to the demonstrated figure a pollution only over a one tide cycle is simulated. The occurring concentration levels have to be reduced by multiplying them by the rate of decay. An integration then gives the desired curve of a non-conservative pollutant at the estimated point of the estuary. The time increment of integration in this operation is just one tidal cycle.

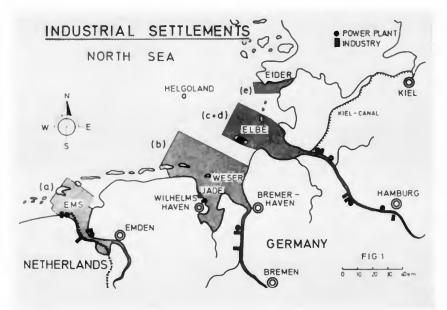
2361

CONCLUSIONS

Froudian tidal modelling besides two dimensional mathematical representation has proved to be a useful method to get information about the concentration levels of pollutants spreading into an area with tidal actions. The decay of non-conservative pollutants can be evaluated by using a decay curve. Distortion with scales of 1:500/1:100 and the use of special artificial roughness elements seem to counterbalance the effects of a differently turbulent diffusion in vertical and horizontal directions which is predicted by theory. The flow pattern in a model should be rough turbulent.

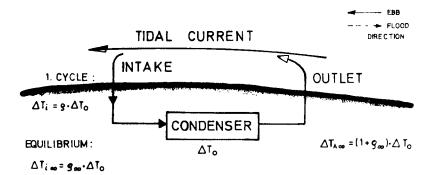
REFERENCES

- [1] CRICKMORE, 1972, Tracer tests of eddy diffusion in field and model, Proc. of the ASCE HY 10.
- [2] OHLMEYER/VOLLMERS, 1973, Thermal and sewage pollution in tidal areas, Proc. of the 15th IAHR Congress, Vol. 2, Istanbul.



2362

DIRECT RECIRCULATION





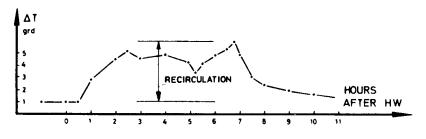


FIG. 3 INCREASING TEMPERATURES DURING EBB CURRENT





THE POWER PLANTS MODEL FIG. 4

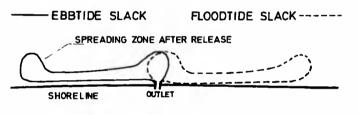
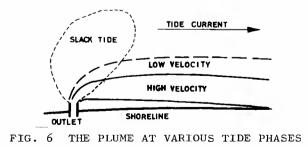


FIG. 5 THE SHAPE OF THE PLUME



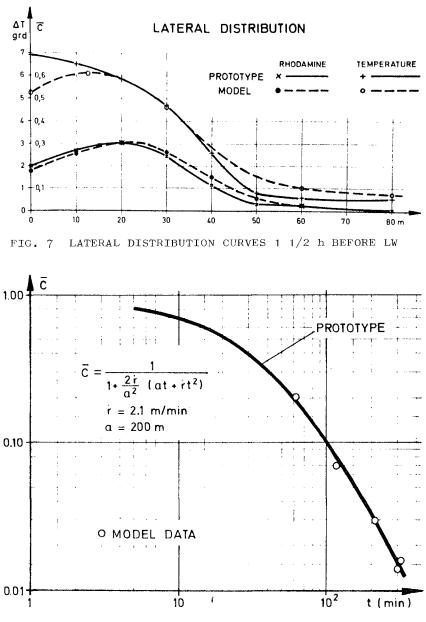


FIG. 8 DECREASING CONCENTRATION MAXIMUM OF A DYE PATCH IN PROTOTYPE AND MODEL



FIG. 9 THE DYE PATCH FROM 600 ft HIGHT

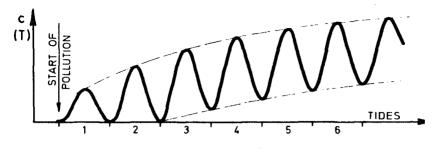


FIG. 10 INCREASING CONCENTRATION (OR TEMPERATURE) CURVE

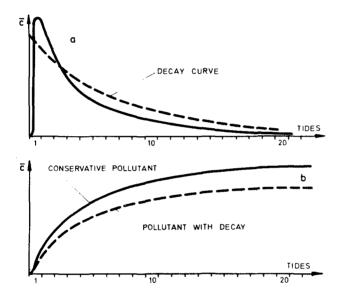


FIG. 11 CONCENTRATION CURVE WITH ONE TIDE CYCLE POLLUTION